



# Intrinsically Water-Stable Keratin Nanoparticles and Their *in Vivo* Biodistribution for Targeted Delivery

Helan Xu,<sup>†,‡</sup> Zhen Shi,<sup>†,§</sup> Narendra Reddy,<sup>†</sup> and Yiqi Yang<sup>\*,†,‡,§,||</sup>

<sup>†</sup>Department of Textiles, Merchandising and Fashion Design, and <sup>||</sup>Department of Biological Systems Engineering, University of Nebraska—Lincoln, 234 Home Economics Building, Lincoln, Nebraska 68583-0802, United States

<sup>‡</sup>Key Laboratory of Science and Technology of Eco-Textiles, Ministry of Education, Donghua University, Shanghai 201620, People's Republic of China

<sup>§</sup>Key Laboratory of Eco-Textiles, Ministry of Education, College of Textiles and Clothing, Jiangnan University, 1800 Lihu Road, Wuxi, Jiangsu 214122, People's Republic of China

**ABSTRACT:** Highly water-stable nanoparticles of around 70 nm and capable of distributing with high uptake in certain organs of mice were developed from feather keratin. Nanoparticles could provide novel veterinary diagnostics and therapeutics to boost efficiency in identification and treatment of livestock diseases to improve protein supply and ensure safety and quality of food. Nanoparticles could penetrate easily into cells and small capillaries, surpass detection of the immune system, and reach targeted organs because of their nanoscale sizes. Proteins with positive and negative charges and hydrophobic domains enable loading of various types of drugs and, hence, are advantageous over synthetic polymers and carbohydrates for drug delivery. In this research, the highly cross-linked keratin was processed into nanoparticles with diameters of 70 nm under mild conditions. Keratin nanoparticles were found supportive to cell growth via an *in vitro* study and highly stable after stored in physiological environments for up to 7 days. At 4 days after injection, up to 18% of the cells in kidneys and 4% of the cells in liver of mice were penetrated by the keratin nanoparticles.

**KEYWORDS:** keratin, nanoparticles, dissolution, *in vivo*, targeted delivery, biodistribution

## INTRODUCTION

Livestock is the major resource to supply protein in the human diet and contributes to an important portion of the global economy. Diseases are major setbacks in livestock production and necessitate improvement from the traditional methods of diagnosis and therapeutic approaches. Nanoparticles provide novel veterinary diagnostics and therapeutics to boost the efficiency in identification and treatment of diseases to reduce loss of animals and improve protein supply and food security.

Nanoparticles have received considerable attention in controlled and sustained drug delivery and many other medical applications. In comparison to microsphere vehicles, nanoparticles possess advantages of having smaller diameters, larger surface area, and better capability to penetrate into cells. Besides, nanoparticles are preferred for treating tumors because they tend to accumulate in tumors because of the “enhanced permeation and retention” effect.<sup>1</sup> Nanoparticles could be prepared from both organic and inorganic materials. Functional inorganic nanoparticulate delivery systems, such as titania nanoparticles,<sup>2–4</sup> have been developed as a drug delivery system and wound-healing applications in biomedical areas.

However, natural biopolymers have attracted increasing attention as nanoparticulate drug delivery vehicles,<sup>5</sup> because of their biocompatibility and large availability. With inherent biodegradability, natural biopolymers do not accumulate in organs like non-biodegradable materials, such as carbon nanotubes<sup>6</sup> or metal nanoparticles.<sup>7</sup>

Among natural polymers, proteins could be preferred in drug loading and sustainable and targeted drug delivery because of their structural characteristics. Proteins could carry positive or

negative charges at pH values below or above their isoelectric points, respectively, and, thus, could facilitate loading of drugs with different charges. Moreover, proteins had hydrophobic domains in their molecular structures and, hence, could attract hydrophobic therapeutics, such as water-insoluble drugs. Thus far, proteins, such as casein,<sup>8,9</sup> lactoglobulin,<sup>10</sup> gelatin,<sup>11</sup> and zein,<sup>12</sup> have been fabricated into nanoparticles for drug delivery.<sup>13</sup>

However, proteins currently studied for medical applications had poor stability under aqueous environments. Physical and chemical modifications were two commonly used approaches to improve water stability of protein nanoparticles. For example, water stability of zein nanoparticles was improved after physical incorporation of charged macromolecule sodium caseinate.<sup>14</sup> Gelatin nanoparticles needed to be chemically cross-linked for controlled release of therapeutics or DNA.<sup>15</sup> However, the two cross-linking methods had their own disadvantages in applications. Physical cross-linking might be easily disturbed by ions and pH in the aqueous environments,<sup>16</sup> while chemical cross-linking might have the issues of toxicity of remaining cross-linkers<sup>17</sup> or low cross-linking efficiency of nontoxic cross-linkers.<sup>18</sup> To avoid the problems associated with cross-linking, using an intrinsically water-stable protein could be an alternative.<sup>19,20</sup>

**Received:** May 13, 2014

**Revised:** August 20, 2014

**Accepted:** August 31, 2014

**Published:** September 1, 2014

Keratin, the major protein in poultry feathers, hairs, and horns of animals, was water-stable and biocompatible and could be a promising biomaterial for medical applications. Keratin has molecular structures similar to collagen, the prominent protein in native extracellular matrices (ECMs). Furthermore, tripeptides “Arg-Gly-Asp” (RGD) and “Leu-Asp-Val” (LDV) existing in keratin molecules could bind with cell surface ligands and promote cell adhesion on keratin-based materials.<sup>21</sup> In addition, because of the highly cross-linked molecular structures attributed to the 7% cysteine in the amino acid components,<sup>21</sup> keratin might not suffer from poor water stability, the prominent problem that restricted biomedical applications of many proteins.

Because of its intrinsic water stability, keratin is advantageous over other proteins as nanoparticles. As a satisfactory biomaterial,<sup>22</sup> keratin was used to coat silver nanoparticles to improve their water stability.<sup>23</sup> Keratin has been fabricated into microparticles<sup>24</sup> and nanoparticles with polyethylene glycol grafting or using toxic solvent.<sup>25</sup> A better method should be developed, and the biodistribution should be investigated for drug delivery purposes.

## MATERIALS AND METHODS

**Materials.** Chicken feather barbs were provided by Featherfiber Corporation, Nixa, MO. Sodium bisulfite (98.0%), sodium hydroxide, hydrochloric acid, and ethylene glycol were purchased from AMRESCO LLC, Solon, OH. Purity of chemicals was considered in all of the calculations of concentrations.

**Preparation of Nanoparticles.** Chicken feathers were washed with reflux of ethanol in a Soxhlet extractor for 12 h to remove lipid and other impurities, followed by rinsing in distilled water 3 times to remove water-soluble impurities. After drying under 50 °C, the cleaned chicken feathers were hydrolyzed using 0.1 M sodium hydroxide at a ratio of 15:1 with sodium bisulfite (30% on weight of feathers) for 2 h at 80 °C. Hydrochloric acid was added to precipitate hydrolyzed feather keratin. The dispersion was centrifuged at 8000 rcf for 20 min, and subsequently, the obtained precipitated keratin was washed using distilled water 3 times. The feather keratin was dried under 50 °C and pulverized into powder.

To prepare nanoparticles, the obtained keratin powder was dissolved in ethylene glycol at designated concentrations (1, 2, 3, 4, 5, 10, and 20%, w/w) under room temperature. To precipitate keratin microparticles, ethylene glycol solution of keratin was added to distilled water with a weight ratio of keratin/water at 1:500. To further break the keratin microparticles into nanoparticles, 30 min of ultrasonication was applied using an ultrasonic processor (VCX 500:500 W, Sonics & Materials, Newton, CT) with an amplitude of vibration at 40%. At last, the dispersion of keratin nanoparticles were dialyzed (molecular weight cutoff of 7000) against distilled water for 4 days to remove ethylene glycol. The concentration of the keratin nanoparticles was adjusted via evaporation under reduced pressure.

**Size Measurement via Dynamic Light Scattering.** The sizes and  $\zeta$  potential of keratin nanoparticles were measured on a Delsa Nano C particle analyzer (Beckman Coulter, Inc., Brea, CA) at least 1 h after particle formation. Sodium hydroxide and hydrochloric acid were used to adjust pH values of the dispersion to study the effects of pH on the size and surface charge of keratin nanoparticles. At least three measurements from separate samples were performed for each condition, and the average and standard deviation of the data are reported.

**Transmission Electron Microscopy (TEM).** Nanoparticle dispersion was placed on the copper mesh, dried, and then observed under a transmission electron microscope (Hitachi H7500 transmission electron microscope, Hitachi, Inc., Parlin, NJ).

**Crystallinity Analysis.** An X-ray diffraction (XRD) study was carried out on raw chicken feathers and freeze-dried keratin nanoparticles. The data were obtained using a Rigaku SmartLab X-

ray diffractometer with Bragg–Brentano parafocusing geometry, a diffracted beam monochromator, and a conventional copper target X-ray tube set ( $\lambda = 1.54 \text{ \AA}$ ) to 40 kV and 44 mA at 26 °C. Diffraction intensities were recorded with  $2\theta$  ranging from 3° to 40° at a scan speed of 0.02°/s.

**Stability of the Nanoparticles.** To evaluate the dimensional stability, physiological conditions of pH 7 and 37 °C and pH 6 and 37 °C and storage conditions of pH 2 and 4 °C were used to store the keratin nanoparticle dispersion with a concentration of 1 wt %. At designated time points, sizes of keratin nanoparticles were measured in the particle size analyzer. Three samples were measured for each condition to obtain average and standard deviation.

**In Vitro Study.** To evaluate the biocompatibility, dispersion of keratin nanoparticles (10% on weight of the medium) was added to Dulbecco's modified low-glucose Eagle's medium (DMEM, Sigma-Aldrich, St. Louis, MO). NIH 3T3 mouse fibroblast cells (ATCC CRL-1658, Manassas, VA) with a seeding density of  $1 \times 10^5$  cells/mL were cultured in humidified 5% CO<sub>2</sub> at 37 °C for 5 days. After every 24 h, the metabolic activity of the cells were analyzed using the MTS assay (Promega, Madison, WI) according to standard procedures with a multi-well plate Multiskan reader (Thermo Scientific, Waltham, MA). To prepare control samples, aliquots of distilled water with the same volume of keratin nanoparticle dispersion were added to the cell culture medium. For each data point, 6–9 replication experiments were conducted. Cells cultured in DMEM without keratin nanoparticles were used as a control.

**In Vivo Study.** Biodistribution of keratin nanoparticles in mice was studied. The nanoparticles were first labeled with fluorescein isothiocyanate (FITC, Sigma-Aldrich, St. Louis, MO) in dimethyl sulfoxide (DMSO) with the addition of pH 9.5 carbonate–bicarbonate buffer in the dark. Free FITC was removed after dialyzed against distilled water for 4 days. The concentration of the FITC–keratin dispersion was readjusted to 100 mg/mL via evaporation under reduced pressure.

Mice were injected intravenously with 0.17 mL of dispersion of keratin nanoparticles (1%, w/w) every 24 h for up to 5 days. The mice were sequentially sacrificed 24 h after injection for up to 5 days. Mice sacrificed after the first 24 h had one injection of the nanoparticles; mice sacrificed after 48 h had two injections; etc. At the required time, mice were euthanized using CO<sub>2</sub> to collect the major organs, including liver, kidney, spleen, heart, and lungs. Organs stored in RPMI solution at 4 °C were analyzed in 5 h after collection. All experiments were carried out according to the Institutional Animal Care and Use Committee (IACUC)-approved protocol, and two mice were sacrificed for each time point.

The organ tissues were minced using a 70  $\mu$ m cell strainer (Falcon, Tewksbury, MA) to obtain single-cell suspension in RPMI solution. For each organ, an aliquot of 500  $\mu$ L of cell suspension was measured on the flow cytometer (BD Accuri, Franklin Lakes, NJ). The population of single cells was defined in a plot of 90° side scattering (SSC) versus forward scattering (FSC), and the percentage of nanoparticle-loaded cells was counted by measuring the fluorescence signal in the green fluorescence channel (FL1).

**Statistical Analysis.** All of the data obtained were analyzed by the one-way analysis of variance with the Scheffé test with a confidence interval of 95%. For characterizations of keratin nanoparticles, at least four specimens were measured or analyzed for each sample under one treatment. A statistically significant difference was indicated with a *p* value smaller than 0.05. The data in the figures labeled with different numbers or characters indicated significant differences among different conditions.

## RESULTS AND DISCUSSION

**Characterizations of Keratin Nanoparticles.** Morphologies of the nanoparticles were shown in the TEM image in Figure 1. The dark shade indicated that the particles had solid structures. The particle sizes varied from around 50 to 130 nm. The sizes of keratin nanoparticles made them not easily being immediately filtered via kidney, because it has been reported

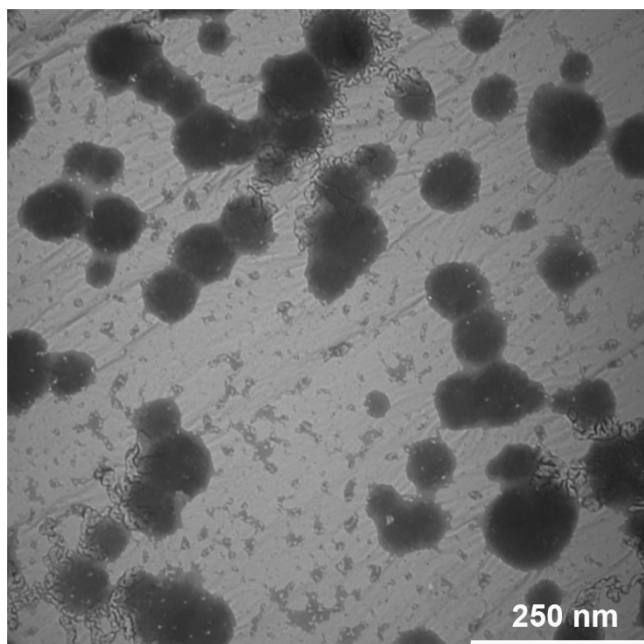


**Figure 1.** Morphologies of keratin nanoparticles in a TEM image showing the diameters from 50 to 130 nm and solid structures.

that nanoparticles with diameters smaller than 5.5 nm could be completely removed from the blood and then body.<sup>26</sup>

Figure 2 shows that the particle sizes obtained from particle analyzer measurement did not change significantly as the

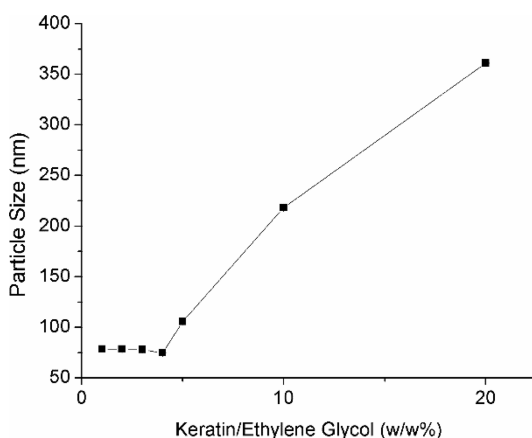


**Figure 2.** Effect of keratin/ethylene glycol ratio on the particle sizes of keratin nanoparticles. Keratin was dissolved in ethylene glycol at concentrations of 1, 2, 3, 4, 5, 10, and 20% based on the weight of ethylene glycol.

keratin concentration increased from 1 to 5% and then increased significantly from less than 100 nm to larger than 350 nm. The average diameter of 70 nm measured using the particle size analyzer was consistent with the results of TEM observation, as shown in Figure 1. A lower concentration of keratin resulted in less polypeptides that could wrap on keratin nanoparticles to increase the particle size. However, agglomeration tended to occur while the keratin concentration increased.

Figure 3 demonstrates that the hydrolyzed keratin had an isoelectric point (PI) of around 4.4 and a strong net surface charge at high or low pH values.  $\zeta$  potential of keratin

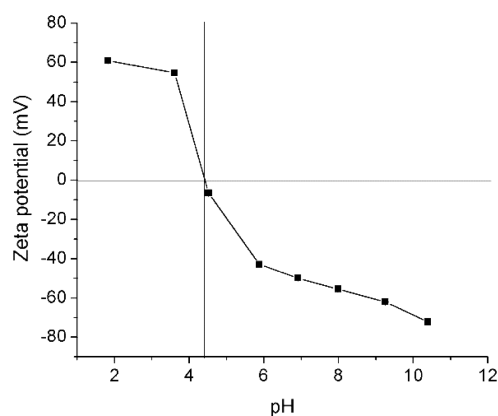


**Figure 3.**  $\zeta$  potential of keratin nanoparticles. Sodium hydroxide solution and hydrochloric acid solution were used to adjust pH values of the keratin dispersion before ultrasonication. The nanoparticles were stabilized for 1 h before measurement.

nanoparticles could increase to higher than 50 mV at pH below 3. A negative charge was shown on the keratin particles at pH values above 6.0, and the  $\zeta$  potential decreased to  $-60$  mV when pH was around 10. The range of surface charge variation reached 120 mV (from 60 to  $-60$  mV) as pH varied from 2.0 to 12.0. The net charge on keratin nanoparticles was much higher than nanoparticles from other proteins, indicating higher potential for keratin to attract adsorbates with opposite charges.<sup>27</sup> Therefore, keratin nanoparticles may serve as good adsorbents to both positively or negatively charged substances.

Figure 4 shows the wide-angle XRD profiles of raw chicken feathers and dry keratin nanoparticles. For both samples, a

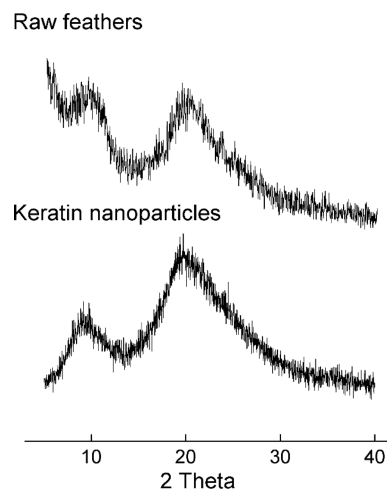


**Figure 4.** XRD spectrogram of keratin nanoparticles and raw feathers.

prominent  $2\theta$  peak at  $20^\circ$  and a minor peak at  $9^\circ$  indicated a typical diffraction pattern of  $\alpha$ -keratin with crystalline spacings of 4.4 and 9.8 Å, respectively. The proportion of the  $2\theta$  peak at  $20^\circ$  increased and that of  $2\theta$  peaks at  $9^\circ$  decreased after dissolution and precipitation of keratin, inferring that raw feathers had a larger amount of more tightly packed crystals than regenerated keratin nanoparticles. A certain degree of damage might occur to the original molecular structures during preparation of nanoparticles.

**Stability of Keratin Nanoparticles.** Figure 5 shows that the sizes of keratin nanoparticles increased from 75 to 130 nm as pH increased from 2 to 5 and then decreased from 130 nm



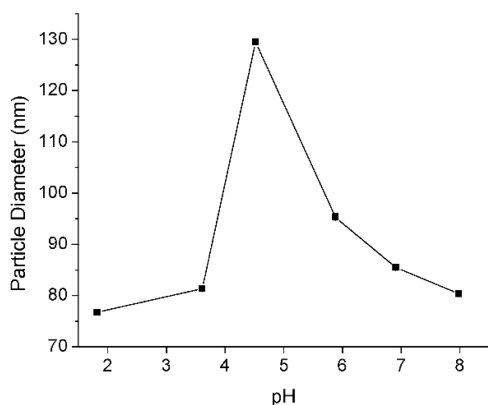


**Figure 5.** Effect of pH on the particle sizes of keratin nanoparticles. Sodium hydroxide solution and hydrochloric acid solution were added to the dispersion before ultrasonication to adjust pH values of the keratin dispersion. The nanoparticles were stabilized for 1 h before measurement.

to less than 85 nm as pH decreased from 5 to 8. The keratin nanoparticles had large diameters at pH similar to pI, because lower surface charge reduced electrical repulsion among nanoparticles and, thus, induced aggregation of small nanoparticles into larger nanoparticles. However, under physiological pH of 7.4 and storage pH of 2, keratin nanoparticles did not show hydrodynamic diameters larger than 100 nm.

Figure 6 indicated that keratin nanoparticles increased in the first 8 h and stabilized for up to 50 h when stored in phosphate-

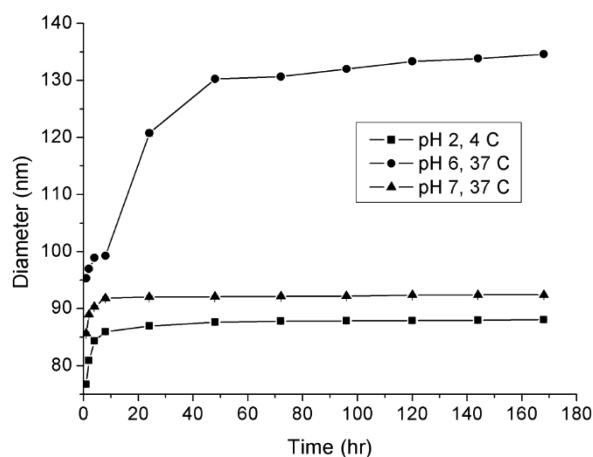


**Figure 6.** Influence of pH and temperature on the sizes of the keratin nanoparticles between 0 and 170 h. The diameters of keratin nanoparticles increased rapidly during the first 10 h and became stable at pH 2 under 4 °C and pH 7 under 37 °C.

buffered saline (PBS) medium. Keratin nanoparticles were highly stable at pH 2 under 4 °C, moderately stable at pH 7 under 37 °C, but unstable at pH 6 under 37 °C. Instability of the nanoparticles at a higher temperature should be due to the higher mobility, and therefore, chances of collision between particles could lead to agglomeration. Under the same temperature, pH 6 was closer to pH 4.5 compared to pH 7, suggesting weaker electrostatic repulsion among the keratin nanoparticles, as indicated in Figure 2, and therefore, better stability was seen at pH 7. However, even under high temperatures at pH 6, the diameters of keratin nanoparticles were still below 150 nm, indicating that the nanoparticles had

remarkable water stability. The intrinsically high cross-linking degree of keratin might contribute to the water stability of the keratin nanoparticles.<sup>27</sup>

**In Vitro Study for Biocompatibility.** The effects of keratin nanoparticles on cell growth and proliferation *in vitro* are shown in Figure 7. Cells in the culture medium containing keratin

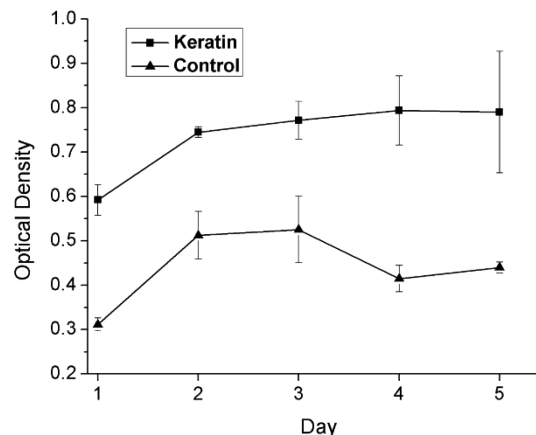


**Figure 7.** Comparison of the optical densities of mouse fibroblast cells with and without nanoparticles based on the MTS assay. The cells were cultured at 37 °C for 5 days.

nanoparticles showed continued proliferation of cells from day 1 to day 5, while the cells in culture medium without any additional additives showed maximum population on days 2 and 3, followed with a decrease on days 4 and 5. Keratin nanoparticles could hydrolyze into peptides and amino acids in the culture medium that could act as a nutrient to support cell growth, leading to higher proliferation.

**In Vivo Study for Biodistribution.** As shown in Figure 8, keratin nanoparticles were predominantly found in the kidneys,

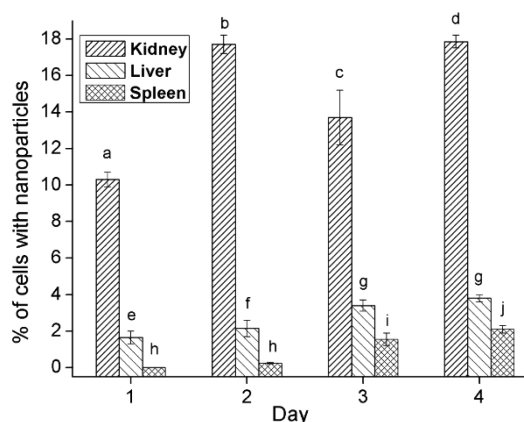


**Figure 8.** Comparison of the percentage of cells containing nanoparticles detected in kidneys, liver, and spleen in mice using flow cytometer after 1, 2, 3, and 4 days of injection. The uptake of nanoparticles did not increase continuously in kidneys but increased gradually in liver and spleen.

followed by liver and spleen in mice. The amount of nanoparticles in kidneys was not affected by dosage, while the amount of the nanoparticles in liver and spleen gradually increased as the dosage increased. Nanoparticles with diameters up to about 5.5 nm could be completely filtered by kidneys.<sup>28</sup> Keratin nanoparticles had significantly larger average diameter

and were probably trapped in the kidneys before they were degraded into diameters smaller than 5.5 nm. The undegraded particles are removed via hepatic clearance through liver, which clears nanoparticles in the range of 10–20 nm.<sup>29</sup> Therefore, considerable amounts of nanoparticles were also found in the liver. Fewer nanoparticles could reach the spleen after being accumulated or filtered in the kidneys and liver. Successive injections were made every 24 h to ensure that sufficient nanoparticles were available to reach the targeted organs. After multiple injections, the amount of nanoparticles did not change significantly in kidneys. However, the quantity of nanoparticles slightly increased in liver and spleen in 2 days but also leveled off at the third and fourth days. The phenomenon suggested that the keratin nanoparticles could effectively degrade in the body. Keratin nanoparticles could be effective drug delivery vehicles to target kidney and liver for sustained release.

Cross-linking degrees of proteins might markedly affect the biodistribution of nanoparticles in different organs. Nanoparticles from highly cross-linked keratin with 7% cysteine<sup>30</sup> showed a similarly high content of accumulation in kidneys compared to those from other highly cross-linked protein, such as wheat glutenin.<sup>31</sup> However, nanoparticles from zein with a trace content of cysteine among its amino acids<sup>32</sup> were mainly found in liver.<sup>33</sup> In nature, keratin is a protein that takes a considerably long time to degrade because of the cross-linked structure. Even with partially destroyed physical structures, as indicated by the XRD results in Figure 4, the remaining cross-linkage still might render the keratin nanoparticles stable at physiological pH, as shown in Figure 6. It could be inferred that the cross-linking degree of proteins might have major effects on the water stability and enzymatic degradation rate of nanoparticles in physiological environments and, thus, might influence the biodistribution of protein nanoparticles.

In this research, the highly cross-linked keratin was developed into nanoparticles at around 70 nm via a phase separation and ultrasonication method. The influence of conditions, such as ratios of keratin/ethylene glycol and pH of dispersion on the particle sizes, was investigated. The isoelectric point of keratin was around pH 4.4. The keratin nanoparticles were highly stable after stored in physiological pH of 7 and storage condition of pH 2. The *in vitro* study indicated that keratin nanoparticles supported the attachment and proliferation of fibroblast cells. After injection into mice, it was found that up to 18% of the cells in kidneys and 4% of the cells in liver of mice were penetrated by the keratin nanoparticles. In summary, keratin nanoparticles could be potential vehicles for efficient drug delivery in treatments of livestock diseases.

## AUTHOR INFORMATION

### Corresponding Author

\*Telephone: +001-402-472-5197. Fax: +001-402-472-0640. E-mail: yyang2@unl.edu.

### Funding

This research was financially supported by the Agricultural Research Division at the University of Nebraska—Lincoln, the United States Department of Agriculture (USDA) Hatch Act, the Multistate Research Project S-1054 (NEB 37-037), the Nebraska Environmental Trust (13-142), and the Key Scientific and Technological Projects of Science and Technology Commission of Shanghai Municipality (12JC1400300). Financial support provided to Zhen Shi through the Program for Changjiang Scholars and Innovative Research Team in

University (IRT1135) at Jiangnan University, the Scientific Support Program of Jiangsu Province (BE2011404), the Graduate Student Innovation Plan of Jiangsu Province (CX10B\_222Z), and the Doctor Candidate Foundation of Jiangnan University (JUDCF10004) is also thankfully acknowledged.

### Notes

The authors declare no competing financial interest.

## ACKNOWLEDGMENTS

The authors thank Dr. Han Chen for his help in TEM and Zhuangzhuang Ma for her help in XRD.

## REFERENCES

- (1) Iyer, A. K.; Khaled, G.; Fang, J.; Maeda, H. Exploiting the enhanced permeability and retention effect for tumor targeting. *Drug Discovery Today* **2006**, *11*, 812–818.
- (2) Sunkara, B. K.; Misra, R. D. K. Enhanced antibactericidal function of W<sup>4+</sup>-doped titania-coated nickel ferrite composite nanoparticles: A biomaterial system. *Acta Biomater.* **2008**, *4*, 273–283.
- (3) Huang, H.; Yuan, Q.; Shah, J. S.; Misra, R. D. K. A new family of folate-decorated and carbon nanotube-mediated drug delivery system: synthesis and drug delivery response. *Adv. Drug Delivery Rev.* **2011**, *63*, 1332–1339.
- (4) Zhang, J.; Misra, R. D. K. Magnetic drug targeting carrier encapsulated with thermosensitive smart polymer: Core-shell nanoparticle carrier and drug release response. *Acta Biomater.* **2007**, *3*, 838–850.
- (5) Xu, W.; Yang, Y. Drug release and its relationship with kinetic and thermodynamic parameters of drug sorption onto starch acetate fibers. *Biotechnol. Bioeng.* **2010**, *105*, 814–822.
- (6) Yang, S.-T.; Wang, X.; Jia, G.; Gu, Y.; Wang, T.; Nie, H.; Ge, C.; Wang, H.; Liu, Y. Long-term accumulation and low toxicity of single-walled carbon nanotubes in intravenously exposed mice. *Toxicol. Lett.* **2008**, *181*, 182–189.
- (7) Nel, A.; Xia, T.; Mädler, L.; Li, N. Toxic potential of materials at the nanolevel. *Science* **2006**, *311*, 622–627.
- (8) Zhen, X.; Wang, X.; Xie, C.; Wu, W.; Jiang, X. Cellular uptake, antitumor response and tumor penetration of cisplatin-loaded milk protein nanoparticles. *Biomaterials* **2013**, *34*, 1372–1382.
- (9) Elzoghby, A. O.; Abo El-Fotoh, W. S.; Elgindy, N. A. Casein-based formulations as promising controlled release drug delivery systems. *J. Controlled Release* **2011**, *153*, 206–216.
- (10) Teng, Z.; Li, Y.; Luo, Y.; Zhang, B.; Wang, Q. Cationic  $\beta$ -lactoglobulin nanoparticles as a bioavailability enhancer: Protein characterization and particle formation. *Biomacromolecules* **2013**, *14*, 2848–2856.
- (11) Ding, D.; Zhu, Z.; Liu, Q.; Wang, J.; Hu, Y.; Jiang, X.; Liu, B. Cisplatin-loaded gelatin-poly(acrylic acid) nanoparticles: Synthesis, antitumor efficiency in vivo and penetration in tumors. *Eur. J. Pharm. Biopharm.* **2011**, *79*, 142–149.
- (12) Xu, H.; Jiang, Q.; Reddy, N.; Yang, Y. Hollow nanoparticles from zein for potential medical applications. *J. Mater. Chem.* **2011**, *21*, 18227–18235.
- (13) Elzoghby, A. O. Gelatin-based nanoparticles as drug and gene delivery systems: Reviewing three decades of research. *J. Controlled Release* **2013**, *172*, 1075–1091.
- (14) Luo, Y.; Teng, Z.; Wang, T. T.; Wang, Q. Cellular uptake and transport of zein nanoparticles: Effects of sodium caseinate. *J. Agric. Food Chem.* **2013**, *61*, 7621–7629.
- (15) Elzoghby, A. O.; Saad, N. I.; Helmy, M. W.; Samy, W. M.; Elgindy, N. A. Ionically-crosslinked milk protein nanoparticles as flutamide carriers for effective anticancer activity in prostate cancer-bearing rats. *Eur. J. Pharm. Biopharm.* **2013**, *85*, 444–451.
- (16) Pawar, S. N.; Edgar, K. J. Alginate derivatization: A review of chemistry, properties and applications. *Biomaterials* **2012**, *33*, 3279–3305.

- (17) Hennink, W.; Van Nostrum, C. Novel crosslinking methods to design hydrogels. *Adv. Drug Delivery Rev.* **2012**, *64*, 223–236.
- (18) Jiang, Q.; Reddy, N.; Yang, Y. Cytocompatible cross-linking of electrospun zein fibers for the development of water-stable tissue engineering scaffolds. *Acta Biomater.* **2010**, *6*, 4042–4051.
- (19) Xu, H.; Cai, S.; Sellers, A.; Yang, Y. Electrospun ultrafine fibrous wheat glutenin scaffolds with three-dimensionally random organization and water stability for soft tissue engineering. *J. Biotechnol.* **2014**, *184*, 179–186.
- (20) Xu, H.; Cai, S.; Sellers, A.; Yang, Y. Intrinsically water-stable electrospun three-dimensional ultrafine fibrous soy protein scaffolds for soft tissue engineering using adipose derived mesenchymal stem cells. *RSC Adv.* **2014**, *4*, 15451–15457.
- (21) Xu, H.; Cai, S.; Xu, L.; Yang, Y. Water-stable three-dimensional ultrafine fibrous scaffolds from keratin for cartilage tissue engineering. *Langmuir* **2014**, *30*, 8461–8470.
- (22) Arai, K.; Naito, S.; Dang, V. B.; Nagasawa, N.; Hirano, M. Crosslinking structure of keratin. VI. Number, type, and location of disulfide crosslinkages in low-sulfur protein of wool fiber and their relation to permanent set. *J. Appl. Polym. Sci.* **1996**, *60*, 169–179.
- (23) Reichl, S. Films based on human hair keratin as substrates for cell culture and tissue engineering. *Biomaterials* **2009**, *30*, 6854–6866.
- (24) Martin, J. J.; Cardamone, J. M.; Irwin, P. L.; Brown, E. M. Keratin capped silver nanoparticles—Synthesis and characterization of a nanomaterial with desirable handling properties. *Colloids Surf., B* **2011**, *88*, 354–361.
- (25) Pedram Rad, Z.; Tavanai, H.; Moradi, A. Production of feather keratin nanopowder through electrospraying. *J. Aerosol Sci.* **2012**, *51*, 49–56.
- (26) Li, Q.; Zhu, L.; Liu, R.; Huang, D.; Jin, X.; Che, N.; Li, Z.; Qu, X.; Kang, H.; Huang, Y. Biological stimuli responsive drug carriers based on keratin for triggerable drug delivery. *J. Mater. Chem.* **2012**, *22*, 19964–19973.
- (27) Choi, H. S.; Liu, W.; Misra, P.; Tanaka, E.; Zimmer, J. P.; Ipe, B. I.; Bawendi, M. G.; Frangioni, J. V. Renal clearance of quantum dots. *Nat. Biotechnol.* **2007**, *25*, 1165–1170.
- (28) Xu, H.; Zhang, Y.; Jiang, Q.; Reddy, N.; Yang, Y. Biodegradable hollow zein nanoparticles for removal of reactive dyes from wastewater. *J. Environ. Manage.* **2013**, *125*, 33–40.
- (29) Katoh, K.; Tanabe, T.; Yamauchi, K. Novel approach to fabricate keratin sponge scaffolds with controlled pore size and porosity. *Biomaterials* **2004**, *25*, 4255–4262.
- (30) Xu, H.; Yang, Y. Controlled de-cross-linking and disentanglement of feather keratin for fiber preparation via a novel process. *ACS Sustainable Chem. Eng.* **2014**, *2*, 1404–1410.
- (31) Reddy, N.; Shi, Z.; Xu, H.; Yang, Y. Development of wheat glutenin nanoparticles and their biodistribution in mice. *J. Biomed. Mater. Res., Part A* **2014**, DOI: 10.1002/jbm.a.35302.
- (32) Gianazza, E.; Viglienghi, V.; Righetti, P. G.; Salamini, F.; Soave, C. Amino acid composition of zein molecular components. *Phytochemistry* **1977**, *16*, 315–317.
- (33) Lai, L. F.; Guo, H. X. Preparation of new 5-fluorouracil-loaded zein nanoparticles for liver targeting. *Int. J. Pharm.* **2011**, *404*, 317–323.